



**HAL**  
open science

## Formation and evolution of F nanobubbles in amorphous and crystalline Si

S. Boninelli, G. Impellizzeri, S. Mirabella, F. Priolo, E. Napolitani, Nikolay Cherkashin, Fuccio Cristiano

### ► To cite this version:

S. Boninelli, G. Impellizzeri, S. Mirabella, F. Priolo, E. Napolitani, et al.. Formation and evolution of F nanobubbles in amorphous and crystalline Si. Applied Physics Letters, 2008, 93 (6), pp.61906 - 171916. 10.1063/1.2969055 . hal-01736061

**HAL Id: hal-01736061**

**<https://hal.science/hal-01736061>**

Submitted on 23 Mar 2018

**HAL** is a multi-disciplinary open access archive for the deposit and dissemination of scientific research documents, whether they are published or not. The documents may come from teaching and research institutions in France or abroad, or from public or private research centers.

L'archive ouverte pluridisciplinaire **HAL**, est destinée au dépôt et à la diffusion de documents scientifiques de niveau recherche, publiés ou non, émanant des établissements d'enseignement et de recherche français ou étrangers, des laboratoires publics ou privés.

## Formation and evolution of F nanobubbles in amorphous and crystalline Si

S. Boninelli, G. Impellizzeri, S. Mirabella, F. Priolo, E. Napolitani, N. Cherkashin, and F. Cristiano

Citation: *Appl. Phys. Lett.* **93**, 061906 (2008); doi: 10.1063/1.2969055

View online: <https://doi.org/10.1063/1.2969055>

View Table of Contents: <http://aip.scitation.org/toc/apl/93/6>

Published by the [American Institute of Physics](#)

---

### Articles you may be interested in

[Evidences of F-induced nanobubbles as sink for self-interstitials in Si](#)

*Applied Physics Letters* **89**, 171916 (2006); 10.1063/1.2364271

[Mechanisms of boron diffusion in silicon and germanium](#)

*Journal of Applied Physics* **113**, 031101 (2013); 10.1063/1.4763353

---



**Scilight**

Sharp, quick summaries **illuminating**  
the latest physics research

Sign up for **FREE!**

**AIP**  
Publishing

## Formation and evolution of F nanobubbles in amorphous and crystalline Si

S. Boninelli,<sup>1,a)</sup> G. Impellizzeri,<sup>1</sup> S. Mirabella,<sup>1</sup> F. Priolo,<sup>1</sup> E. Napolitani,<sup>2</sup> N. Cherkashin,<sup>3</sup> and F. Cristiano<sup>4</sup>

<sup>1</sup>MATIS CNR-INFN and Dipartimento di Fisica ed Astronomia, Università di Catania, Via Santa Sofia 64, 95123 Catania, Italy

<sup>2</sup>MATIS CNR-INFN and Dipartimento di Fisica, Università di Padova, Via F. Marzolo 8, 35131 Padova, Italy

<sup>3</sup>CEMES-CNRS, 29, Rue Jeanne Marvig, 31055 Toulouse, France

<sup>4</sup>LAAS-CNRS, 7, Avenue du Colonel Roche, 31077 Toulouse, France

(Received 19 May 2008; accepted 17 July 2008; published online 13 August 2008)

The formation and evolution of F-induced nanobubbles in Si was investigated. Si samples were preamorphized, implanted with F, and partially regrown by solid phase epitaxy (SPE). It is shown that nanobubbles are formed already in the amorphous side of partially regrown samples and are then incorporated in crystalline Si during SPE. The bubbles are interpreted as the result of the diffusion and coalescence of F atoms and dangling bonds already in the amorphous matrix. During high temperature annealing after SPE, F outdiffuses; correspondingly, the bubbles partially dissolve and transform from spherical- to cylinder-shaped bubbles. © 2008 American Institute of Physics. [DOI: 10.1063/1.2969055]

In recent years, the beneficial effects of F on the reduction of B transient enhanced diffusion (TED) in Si have been widely observed. Many efforts, both experimental and theoretical, have been devoted to understand the F behavior in Si and different mechanisms have been proposed to explain the role of F. So far, it has been proved that the reduction of B TED cannot be ascribed to the formation of F-B complexes.<sup>1</sup> Besides, the interaction between F and Si interstitials atoms (Is) cannot be invoked to explain the beneficial effects of F in terms of stabilization of the end of range defects.<sup>2,3</sup> The formation of F-vacancies (V) complexes was also proposed to explain the effect of F on the reduction of boron TED.<sup>4</sup> Indeed, transmission electron microscopy (TEM) revealed the presence of bubbles in crystalline Si (*c*-Si) implanted with BF<sub>2</sub><sup>+</sup>, after thermal annealing at high temperature,<sup>5,6</sup> and positron annihilation spectroscopy evidenced the presence of F-V complexes in *c*-Si, implanted with F.<sup>7,8</sup> Recently, we investigated the role of F-induced bubbles on Is defects in preamorphized Si, revealing the presence, just after solid phase epitaxy (SPE), of a band of cavities acting as efficient traps for Si Is.<sup>9</sup> These evidences are supported by *ab initio* calculations, which have shown that in *c*-Si, F atoms preferentially form complexes with V (indicated as F<sub>*n*</sub>V<sub>*m*</sub>), due to their great ability in saturating Si dangling bonds (dbs), rather than bind with Is or B or F.<sup>10</sup> Indeed, the somewhat high binding energy of these F<sub>*n*</sub>V<sub>*m*</sub> configurations, having all dbs decorated by F, makes them highly stable.<sup>11</sup> In literature, all experiments devoted to the understanding of the F behavior are done with F implanted in crystalline or preamorphized Si matrix. The only experiment realized in amorphous Si (*a*-Si) has been conducted by Nash *et al.*, who studied the transport of F using secondary ion mass spectrometry (SIMS) and showed by TEM that F transport is influenced by F “inclusions.”<sup>12</sup> Clearly, it is now necessary to study the generation of F bubbles in detail and to investigate their

possible formation starting from the amorphous phase.

In this work, we present a study on the formation of F-induced bubbles during SPE. TEM and SIMS analyses reveal that these bubbles already form in *a*-Si, in correspondence of the highly F enriched region. These defects are transferred into the *c*-Si once the amorphous-crystalline (*a-c*) interface advances. The thermal evolution of these F-induced bubbles in recrystallized sample has been investigated and their volume evaluated as a function of thermal treatments.

Silicon samples were prepared by molecular beam epitaxy, containing a Si<sub>1-y</sub>C<sub>y</sub> layer (y=0.005) at a depth of about 800 nm. They were then amorphized from the surface to a depth of ~1 μm by Si implants (5 × 10<sup>15</sup> ions/cm<sup>2</sup> at 500 keV and 2 × 10<sup>15</sup> ions/cm<sup>2</sup> at 40 keV) at liquid nitrogen temperature. F was then implanted in the samples with a dose of 4.4 × 10<sup>15</sup> ions/cm<sup>2</sup> at 75 keV. Finally, samples were annealed at 450 °C for 30 min at 700 °C for 25, 70, or 100 s to induce partial or complete SPE regrowth. In addition, the fully regrown samples were cut into three pieces and further annealed at 800, 900, or 1000 °C for 900 s. The Is released from the end of range defects during annealing are stopped by the Si<sub>1-y</sub>C<sub>y</sub> layer, thus being prevented from arriving at the F-enriched region.<sup>13</sup> The TEM analyses were performed by using a 200 keV JEOL 2010-HC. The F-induced defects are bubbles, which are imaged in defocused off-Bragg bright field conditions to observe the Fresnel-fringe contrast. As this contrast depends on the abrupt change of the mean inner potential at the interface between the bubbles and the Si matrix, it allows the visualization of the whole population of bubbles in both *a*-Si and *c*-Si, within the detection limit of this technique (about 2 nm). The atomic concentration of F was determined by SIMS, using a CAMECA IMS-4f instrument, with a 3 keV, O<sub>2</sub><sup>+</sup> analyzing beam.

In Fig. 1, the kinetics at 700 °C for different times of preamorphized Si implanted with F is reported. All images were obtained by cross-sectional TEM. In the sample annealed for 25 s [Fig. 1(a)] the position of the *a-c* interface is clearly visible at about 250 nm below the surface. A 65 nm wide band of bubbles, whose mean diameter is about 3 nm,

<sup>a)</sup> Author to whom correspondence should be addressed. Present address: Fondazione Istituto Italiano di Tecnologia, Via Morego 30, 16163 Genova, Italy. Electronic mail: simona.boninelli@iit.it.

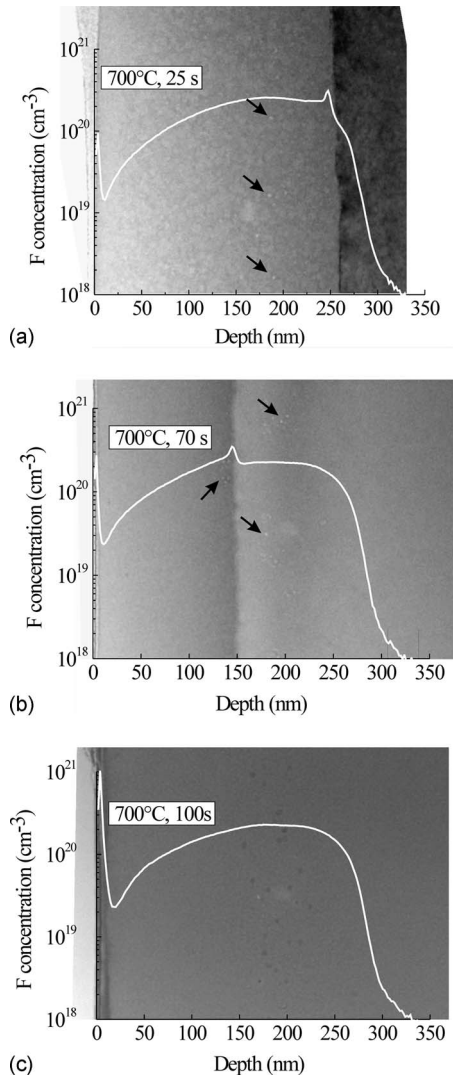


FIG. 1. SIMS  $F$  concentration profile overlapped with TEM cross-sectional view of samples implanted with  $F$  and partially regrown by SPE at  $700\text{ }^{\circ}\text{C}$  for (a) 25 s and (b) 70 s. In (c) the fully regrown sample, after 100 s annealing, is reported. In (a) and (b), the arrows point to some bubbles. The different contrast shown by bubbles in (a) and (b) with respect to (c) depends by the different over- and under-focus imaging conditions used.

is present in the amorphous side centered at a depth of  $\sim 180\text{ nm}$ , while the recrystallized  $\text{Si}$  appears free of defects. After 70 s [Fig. 1(b)] the  $a$ - $c$  interface has shifted at  $\sim 150\text{ nm}$  below the surface and several bubbles with almost unchanged mean sizes, are visible both in the amorphous and crystalline sides. Finally, after 100 s [Fig. 1(c)] the sample is fully recrystallized and a band of larger bubbles (6 nm in diameter) are observed at the same position as before. These results indicate that bubble nucleation is favored in  $a$ - $\text{Si}$ , while bubble growth is enhanced in  $c$ - $\text{Si}$ .

The SIMS  $F$  profile of each sample is superimposed in the cross-sectional image. It has already been shown that partially regrown samples show the characteristic  $F$  segregation peak in the amorphous side of the  $a$ - $c$  interface due to  $F$  atoms, which are forced toward the surface by the moving  $a$ - $c$  interface.<sup>14</sup> Figure 1 shows that the band of bubbles is located around the maximum of the  $F$  concentration profile, clearly suggesting that the mechanism of bubble formation involves  $F$  atoms.

Our results show that bubbles form already in  $a$ - $\text{Si}$  and

that they are incorporated *in toto* during SPE. Amorphous  $\text{Si}$  is represented as a tetrahedrally coordinated configuration without long-range order. The most common defects in  $a$ - $\text{Si}$  are the threefold coordinated  $db$  and the fivefold coordinated floating bonds, represented by hybrid orbitals partially filled by unpaired electrons. It has been demonstrated that these unsaturated bonds are responsible for the passivation of  $\text{Si}$  by  $F$ .<sup>15</sup> Moreover, at high  $F$  concentration the formation of large clusters is favored, as the creation of each  $F$ -saturated  $db$  further lowers the overall energy of the system.<sup>16</sup> This suggests that the early stages of such complexes formation, which prelude to the  $F$ -induced bubbles in  $a$ - $\text{Si}$ , might be originated by the saturation of  $\text{Si}$   $db$  by  $F$ . After the  $700\text{ }^{\circ}\text{C}$ , 25 s annealing, these  $db$ - $F$  complexes grow and evolve toward the formation of clusters, the largest of them being visible by TEM. The thermal annealing at  $700\text{ }^{\circ}\text{C}$  for 70 s, besides favoring the proceeding of the  $a$ - $c$  interface, promotes the further formation of visible bubbles still in the amorphous phase [Fig. 1(b)]. Once formed, these bubbles are extremely stable; thus, they are incorporated directly into the  $c$ - $\text{Si}$  during the passage of the  $a$ - $c$  interface.

In order to investigate the thermal effect on the  $F$  bubbles, the fully regrown samples (post-SPE) were further annealed at 800, 900, and  $1000\text{ }^{\circ}\text{C}$ , for 900 s. In Fig. 2, plan view TEM images of the post-SPE sample [Fig. 2(a)] and of samples further annealed at 900 [Fig. 2(b)] and  $1000\text{ }^{\circ}\text{C}$  [Fig. 2(c)] are reported. The post-SPE sample shows a population of almost spherical bubbles with a mean diameter of about 6 nm. The sample further annealed at the highest temperature ( $1000\text{ }^{\circ}\text{C}$ ) presents again spherical bubbles and a new feature with bubbles elongated in the  $\langle 100 \rangle$  directions, as shown by the corresponding diffraction pattern reported in Fig. 2(d). The mean diameter of spherical bubbles is 3 nm, while the length of the cylindrical bubbles is 10 nm. The sample annealed at  $900\text{ }^{\circ}\text{C}$  presents mainly spherical bubbles (about 80% of the total population of defects) with few cylindrical bubbles, denoting the transition of these defects from the spherical shape toward the cylindrical one. In this case, the mean diameter of the spherical bubbles is 6 nm, while the mean length of the cylindrical ones is 9 nm. Cross-sectional TEM analyses (not shown) evidenced that the defect band enlarges from about 80 nm after SPE to about 170 nm after SPE plus  $1000\text{ }^{\circ}\text{C}$ . Moreover, all cylindrical bubbles shown in Fig. 2(c) display the same diameter value, equal to about 2 nm. By measuring, from Figs. 2(a) and 2(c), size and density of spherical and cylindrical defects, the percentage of volume occupied by the bubbles (in the region where bubbles are present), was evaluated as function of the thermal treatment. The results, reported in Fig. 3 (right vertical axis), show that the percentage of volume occupied by the bubbles decreases from 0.085% after SPE to 0.030% after SPE plus  $1000\text{ }^{\circ}\text{C}$ . These observations suggest that the cylindrical bubbles are the result of a nonconservative evolution, where the spherical bubbles modify themselves after SPE and the length of the cylinders progressively increase. Moreover smaller bubbles, not visible by TEM, are presumably present already after SPE also in regions with a lower  $F$  concentration and grow during post-SPE high temperature annealing forming visible bubbles and producing the observed enlargement of the defect band.

In Fig. 3 (left vertical axis), we reported the  $F$  dose retained in the samples for different thermal treatments, as



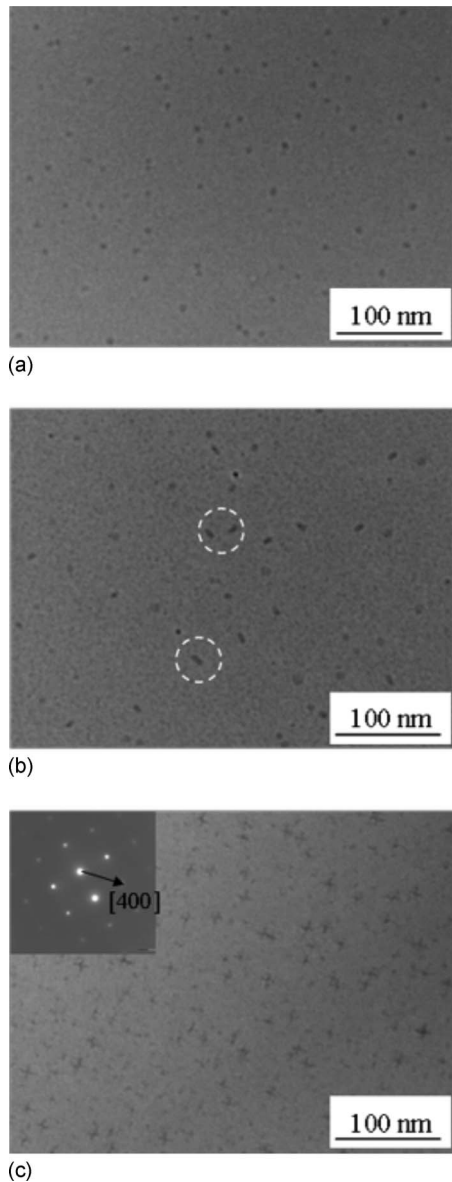


FIG. 2. Plan view images of the (a) sample completely regrown by SPE (700 °C, 100 s) and for post-SPE samples further annealed for 900 s at (b) 900 °C and (c) 1000 °C. In (b) few elongated bubbles are indicated by circles.

measured by SIMS. In detail, the F dose reduces from  $4 \times 10^{15}$  atoms/cm<sup>2</sup> after SPE to  $1 \times 10^{15}$  atoms/cm<sup>2</sup> after SPE plus 1000 °C. By comparing the TEM and SIMS results, it is possible to state that in *c*-Si, while F partially evaporates from the surface, the total volume occupied by bubbles proportionally reduces. Hence we can conclude that bubbles are not only formed but also stabilized by the presence of F, as, once F evaporates, the bands are rearranged and the bubble volume proportionally decreases.

In conclusion, the investigation of F-induced bubble formation in Si during SPE clearly shows the appearance of precursors already in the amorphous phase. This evidence was interpreted in terms of passivation of Si db by F. The growth and coalescence of these F-db complexes lead to the

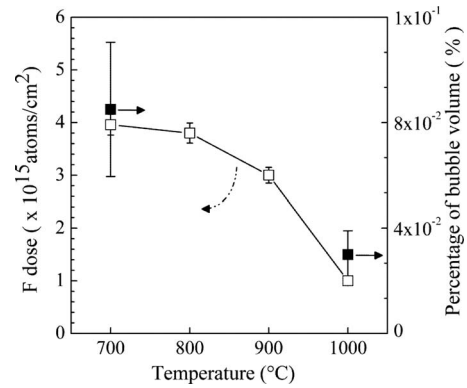


FIG. 3. Behavior of total volume occupied by bubbles per defect band volume (right vertical axis) and dose of incorporated F (left vertical axis) as a function of the post-SPE annealing temperature.

formation of bubbles in the amorphous phase, which are directly transferred in the crystal. Finally we demonstrated that after high temperature annealing a large part of F evaporates from the surface and, at the same time, the defect volume proportionally reduces. These results have important implications for the modeling of F behavior during SPE and its incorporation in *c*-Si, and for its use for point defect engineering in ultrashallow junctions.

We wish to thank C. Percolla and S. Tatì (MATIS CNR-INFM), A. Marino (IMM-CNR), R. Storti (University of Padova), J. Crestou, and C. Crestou (CEMES-CNRS) for technical support. Work at CNRS was partially supported by ESTEEM IP3 project.

- <sup>1</sup>G. Impellizzeri, J. H. R. dos Santos, S. Mirabella, F. Priolo, E. Napolitani, and A. Carnera, *Appl. Phys. Lett.* **84**, 1862 (2004).
- <sup>2</sup>D. F. Downey, J. W. Chow, E. Ishida, and K. S. Jones, *Appl. Phys. Lett.* **73**, 1263 (1998).
- <sup>3</sup>S. Boninelli, F. Cristiano, W. Lerch, S. Paul, and N. E. B. Cowern, *Electrochem. Solid-State Lett.* **10**, H264 (2007).
- <sup>4</sup>M. Diebel, S. Chakravarthi, S. T. Dunham, C. F. Machala, S. Ekbote, and A. Jain, *MRS Symposia Proceedings No. 765* (Materials Research Society, Pittsburgh, 2003), p. D6.15.1.
- <sup>5</sup>J. Narayan, O. W. Holland, W. H. Christie, and J. J. Wortman, *J. Appl. Phys.* **57**, 2709 (1985).
- <sup>6</sup>C. W. Nieh and L. J. Chen, *Appl. Phys. Lett.* **48**, 1528 (1986).
- <sup>7</sup>X. D. Pi, C. P. Burrows, and P. G. Coleman, *Phys. Rev. Lett.* **90**, 155901 (2003).
- <sup>8</sup>P. J. Simpson, Z. Jenei, P. Asoka-Kumar, R. R. Robison, and M. E. Law, *Appl. Phys. Lett.* **85**, 1538 (2004).
- <sup>9</sup>S. Boninelli, A. Claverie, G. Impellizzeri, S. Mirabella, F. Priolo, E. Napolitani, and F. Cristiano, *Appl. Phys. Lett.* **89**, 171916 (2006).
- <sup>10</sup>G. M. Lopez, V. Fiorentini, G. Impellizzeri, S. Mirabella, and E. Napolitani, *Phys. Rev. B* **72**, 045219 (2005).
- <sup>11</sup>M. Diebel and S. T. Dunham, *Phys. Rev. Lett.* **93**, 245901 (2004).
- <sup>12</sup>G. R. Nash, J. F. W. Schiz, C. D. Marsh, P. Ashburn, and G. R. Booker, *Appl. Phys. Lett.* **75**, 3671 (1999).
- <sup>13</sup>E. Napolitani, A. Coati, D. De Salvador, A. Carnera, S. Mirabella, S. Scalse, and F. Priolo, *Appl. Phys. Lett.* **79**, 4145 (2001).
- <sup>14</sup>S. Mirabella, G. Impellizzeri, E. Bruno, L. Romano, M. G. Grimaldi, F. Priolo, E. Napolitani, and A. Carnera, *Appl. Phys. Lett.* **86**, 121905 (2005).
- <sup>15</sup>B. R. Weinberger, H. W. Deckman, E. Yablonovitch, T. Gmitter, W. Kobasz, and S. Garoff, *J. Vac. Sci. Technol. A* **3**, 887 (1985).
- <sup>16</sup>G. M. Lopez and V. Fiorentini, *Appl. Phys. Lett.* **89**, 092113 (2006).